Progress In Electromagnetics Research C, Vol. 35, 237–252, 2013

A MINIMIZED WIDEBAND ANTENNA ARRAY WITH DECOUPLING NETWORKS FOR UHF RFID APPLICATIONS

Tianyu Jia[1, 2], Hua Zhu[1, 2], and Xiuping Li[1, 2, *]

[1]School of Electronic Engineering, Beijing University of Posts and Telecommunications, Beijing 100876, China

[2]State Key Laboratory of Millimeter Waves, Southeast University, Nanjing 210096, China

Abstract—A minimized wideband antenna array is presented for ultra-high frequency (UHF) radio frequency identification (RFID) reader applications. The antenna array consists of two E-shaped patch antennas and a feeding network, with the overall size 200 × 100 × 20 mm^3. The feeding network could effectively decrease the antenna mutual coupling and improve the bandwidth. The measured bandwidth is about 68 MHz (896–964 MHz) under the condition of voltage standing wave ratio (VSWR) less than 2, which covers various RFID bands including North American (902–928 MHz), Chinese (920–925 MHz) and Japanese (952–955 MHz). The average gain is 4.5 dBi in UHF band. The principles of the antenna and the feeding network are also discussed and analyzed in this paper. At last, the key parameters are studied and show the antenna robustness.

1. INTRODUCTION

Radio frequency identification (RFID) system in the ultra-high-frequency (UHF) band (840–960 MHz) has already received considerable attention for various applications, such as identify objects in warehousing, supply chain management, and some other automation processes [1–5]. However, the UHF frequencies standards for RFID applications are different in different countries and regions [6], such as 865–868 MHz in Europe, 902–928 MHz in North America, 920.5–924.5 MHz in China, 920–925 MHz in Singapore and 952–955 MHz in

Received 18 November 2012, Accepted 21 December 2012, Scheduled 28 December 2012
* Corresponding author: Xiuping Li (xpli@bupt.edu.cn).

Japan. Thus, a universal UHF RFID reader should be wide enough to cover several UHF RFID frequencies standards.

Microstrip antenna is commonly designed and used for RFID reader antenna as its structure is able to meet the bandwidth and radiation gain requirements, and a small size will make it suitable for being installed in the reader machines. A series of approaches to improve the microstrip antenna bandwidth and reduce the antenna size have been conducted. Modifying the shape of the radiator patch by slots is the most attractive and effective method to achieve wideband and small size. The successful examples include E-shaped patch antennas [7–10], U-slot patch antennas [11, 12], and V-slot patch antennas [13]. For the E-shaped patch antenna, two parallel slots are incorporated to increase the electrical length and produce wideband antenna [7, 8] or dual-band antenna [9, 10]. Besides, adding a shorting pin is also an effective method to reduce the antenna size [14, 15] as it can notably change the equivalent circuit model of the antenna and reduce the electrical length of the antenna. The principle and results of shorting pins using in the E-shaped patch antenna have been analyzed and proved to be effective to reduce the antenna size [15]. Finally, the defected ground structure (DGS) is also adopted in the antenna design to enhance the radiation gain with improving the input impedance match of the antenna. The study of DGS is applied early, about ten years ago [16, 17], and this method is widely used in recent years into various antenna structures to achieve wide bandwidth or high radiation gain [18–20].

Antenna array can also comprise antenna elements for RFID reader applications. The significant advantage of the antenna array is higher radiation gain and more centered directivities, while the coupling effect between antenna elements is not desired. In order to reduce the mutual coupling between antenna elements closely located within restricted space, different approaches are developed [21–24]. The defected ground structure (DGS) has been used to increase the isolation in dual-polarized and dual-frequency antennas [21, 22]. The electromagnetic band-gap (EBG) structures can suppress the surface wave between antenna elements and reduce the mutual coupling, but they suffer from complexity [23, 24].

In this paper, a series of miniaturization methods including slotting in the patch, shorting pin and DGS were applied into the traditional E-shaped antenna. The antenna achieves good bandwidth and gain performance considering its small size. Moreover, the antenna array composed by two antenna elements is designed for RFID reader applications. In order to reduce the mutual coupling effect and integration, decoupling network and power divider are designed

together as the feeding network under the back of antenna array. Good agreement is achieved between the measured and simulated results. The antenna array can cover various RFID bands, and its radiation gain meets the practical demands.

2. ANTENNA PERFORMANCE AND PRINCIPLE

2.1. Antenna Configuration and Results

The geometry of the proposed antenna element is shown in Figure 1. The antenna consists of an E-shaped patch, a shorting pin, coaxial feeding pin and symmetric slotted ground. The size of the E-shaped patch is $36 \times 36\,\text{mm}^2$ ($\sim 0.12\lambda \times 0.12\lambda$) with unequal parallel slots on it. Both slots have the same width 2 mm, while the lengths are 30 mm and 14 mm, respectively. The patch is placed at a height 20 mm from the ground plane by printed on a FR4 substrate whose thickness is 1.6 mm (relative permittivity $\varepsilon_r = 4.4$, $\tan\delta = 0.02$). The medium between the patch and the ground plane is air. The E-shaped patch is fed at position A and connected to the ground plane at position A′. A shorting pin is also adopted to change the resonant modes of the antenna at position B–B′. The square ground with symmetric slotted by four identical rectangles is printed on the top side of the FR4 substrate, whose size is $100 \times 100\,\text{mm}^2$.

The simulated results of S_{11} and radiation pattern are shown in Figure 2. It is observed that there is a resonance around 920 MHz and that the bandwidth of S_{11} less than −10 dB ranges from 894 to

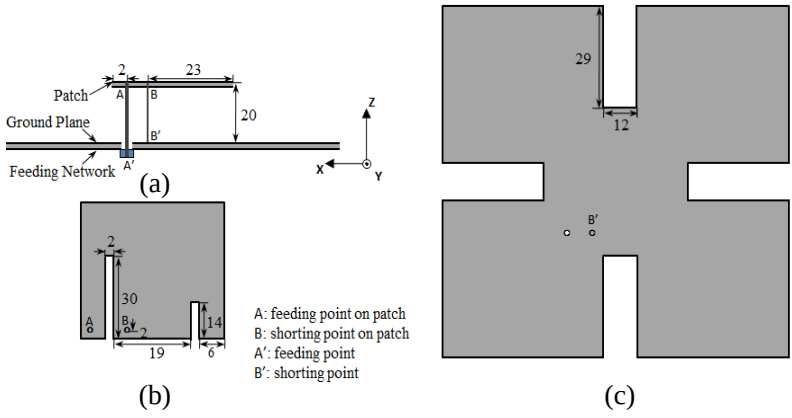

Figure 1. The configuration of the proposed antenna. (a) Side view. (b) E-shaped patch. (c) Ground plane. (Dimensions in mm).

943 MHz (5.33%). The max gain of the antenna is just along z axis, and the gain values are 2.976 dBi and 3.277 dBi at 925 MHz and 950 MHz, respectively.

The bandwidth of the proposed antenna is wide, but it still can be broadened by impedance matching design of the feeding network. Besides, the gain can be improved by antenna array. The two elements antenna array will be introduced in the following.

2.2. Principle of the Proposed Antenna

The equivalent current paths on the patch are shown in Figure 3. As shown in the figure, the structure of the patch contributes to three current paths with different electrical lengths, such as 1, 2 and 3. In order to achieve the resonant mode around 920 MHz, path 1 is designed to be about 120 mm. After adding the length of fed pin and shorting pin, the total electrical length of path 1 is about 160 mm, which is

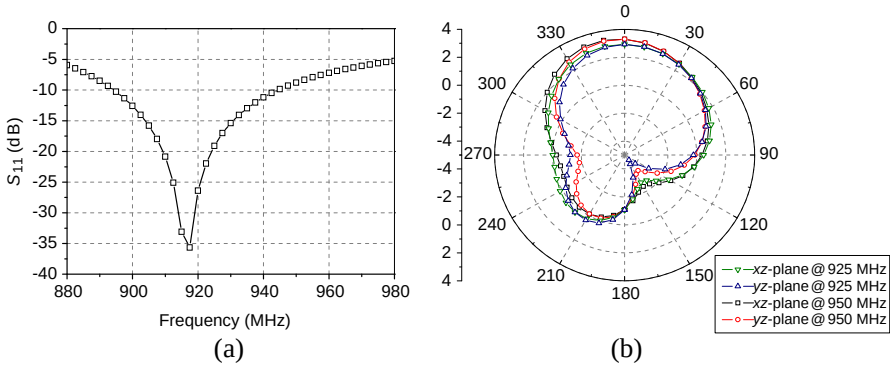

Figure 2. The simulated results of the proposed antenna. (a) S_{11}. (b) Radiation pattern.

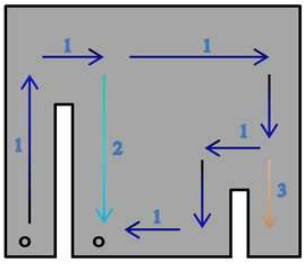

Figure 3. The equivalent current paths on the patch.

about 0.5-wavelength of 900 MHz. Path 2 and path 3 are also created by the slots at the same time, whose total lengths are about 75 mm and 115 mm. These two paths contribute to the resonant mode at around 2 GHz and 5 GHz, which will not be discussed further as the aim band is UHF. In summary, the antenna resonates at 920 MHz based on the patch slots.

The simple symmetric slots on the ground are easy to fabricate and can greatly improve the antenna gain and bandwidth performance. Figure 4 shows different types of current distribution on the ground plane. It is obvious that the symmetric slots in the ground promote current distribution along the edge and increase maximum gain of the proposed antenna.

The effects of slotting for S parameters can be observed in

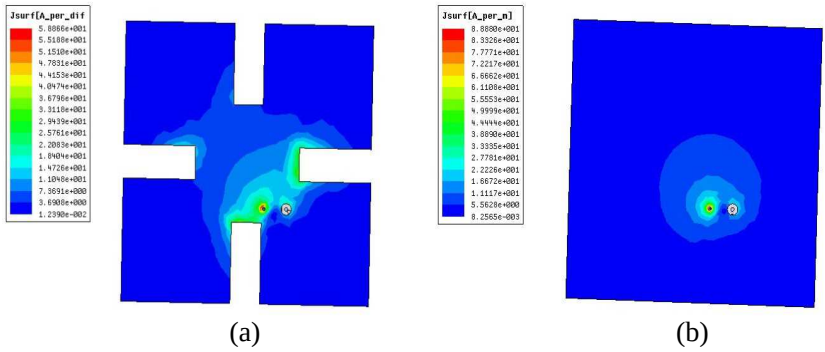

Figure 4. Current distributions on the ground plane. (a) Proposed antenna. (b) Antenna without ground slots.

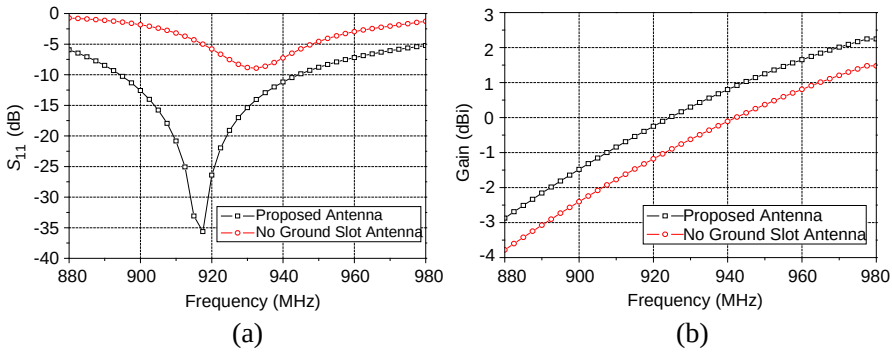

Figure 5. The effects of slotting on the ground. (a) S_{11}. (b) Gain.

Figure 5. The matching performance (S_{11}) of intact ground antenna is always above -10 dB, while the proposed antenna matching is deep to about -35 dB. The maximum gain of the antenna also increases about 1 dBi by these slots.

3. 2×1 ANTENNA ARRAY DESIGN

3.1. Antenna Array

We use two proposed E-shaped patch antenna elements to construct 2×1 antenna array. The simulation model in HFSS is shown in Figure 6. All parameters in the antenna element are maintained. The ground plane of the antenna array is printed on one side of the FR4 substrate and the feeding network on the other. The overall size of the proposed antenna array is $200 \times 100 \times 20\,\text{mm}^3$.

As no extra space is left between these two antenna elements,

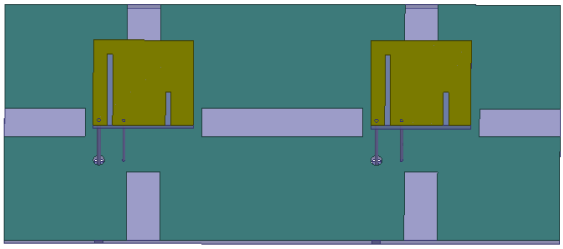

Figure 6. The 2×1 antenna array model in HFSS.

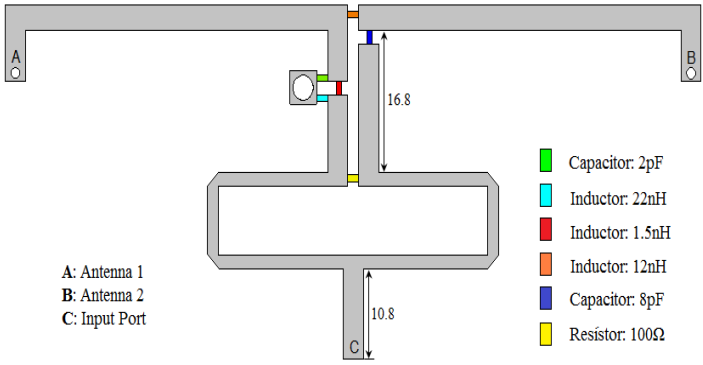

Figure 7. The configuration of feeding network. (Dimensions in mm).

the mutual coupling is serious and greatly decreases the antenna performance. In order to eliminate this terrible coupling, the decoupling and matching network is adopted in the feeding network. Besides, one traditional Wilkinson power divider is utilized for the power feeding. The configuration of the whole feeding network is shown in Figure 7. The overall size of the feeding network is $103 \times 42\,\text{mm}^2$.

In Figure 7, position C is the feeding point through SMA connector, while positions A and B are feeding points for these two antenna elements. The input power will be divided into two equal parts by power divider first, then through decoupling and matching network to the antenna port. The detailed principle and performance of the feeding network will be introduced in the following section.

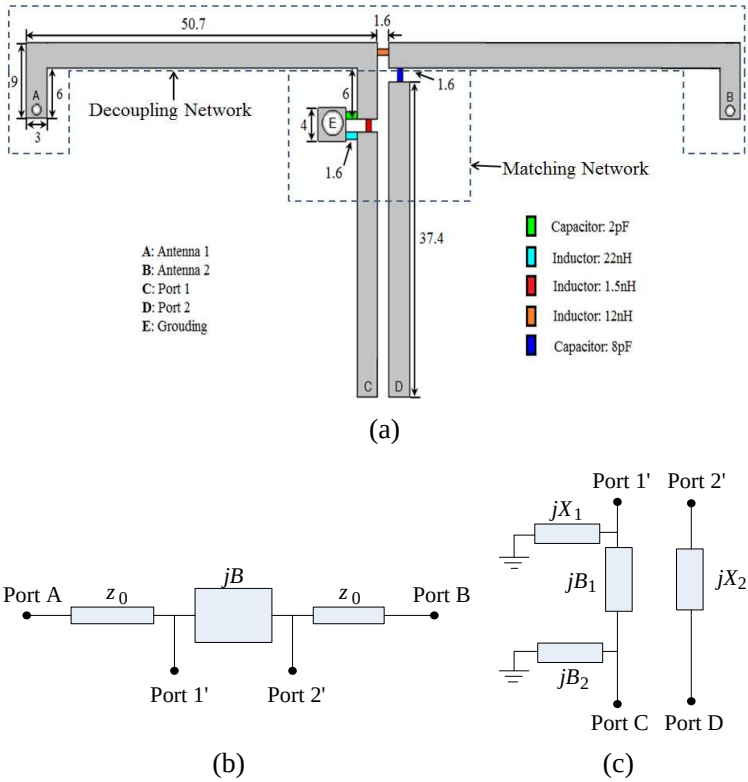

Figure 8. The decoupling and the matching network. (a) Microstrip structure. (b) Decoupling equivalent circuit. (c) Matching equivalent circuit.

3.2. Principle of the Feeding Network

3.2.1. Decoupling and Matching Network

In the proposed antenna array, the two antenna elements have been designed in the area of $200 \times 100\,\text{mm}^2$ and only spaced by $0.31\lambda_0$ (100 mm) at 930 MHz. Decoupling method is necessary to eliminate the serious mutual coupling effect, and there is much previous experience focusing on this area [25, 26]. The configuration of the decoupling network and its equivalent circuit are shown in Figure 8.

Two transmission lines are individually connected to input ports of two strongly coupled antennas in the decoupling network. The width of the metal strip is designed as 3 mm for 50 Ω impedance matching at UHF band. The length of the transmission line is chosen to make the trans-admittance between ports convert into the pure imaginary. A shunt reactive component is then attached in between the transmission line ends to cancel the resultant imaginary trans-admittance.

Besides, π-shaped and L-section network is design to improve input matching for ports 1 and 2, respectively. These two matching networks produce resonant mode at UHF band and significantly broaden the bandwidth of the antenna array. The parameters of decoupling network and matching network elements are calculated and specified in Table 1.

Table 1. Parameters of the decoupling and matching network.

Z_0	B	B_1	B_2	X_1	X_2
50	0.014	0.114	0.008	−11.6	−46.7

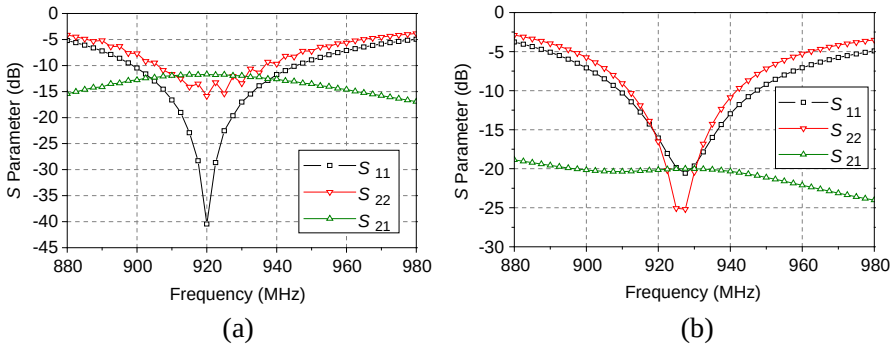

Figure 9. Simulated S parameter results of the decoupling network. (a) S parameter before decoupling. (b) S parameter after decoupling.

Figure 9 shows the decoupling effect of the decoupling network. If the antenna array is simply composed of antenna elements, the coupling effect (S_{21}) between them is around -12 dB in the working band. Besides, the bandwidth of the second antenna element (S_{22}) has also been decreased by the coupling, as shown in Figure 9(a). With the decoupling and matching network, the bandwidth of the two antenna is improved, and the coupling (S_{21}) is decreased to around -20 dB, as shown in Figure 9(b).

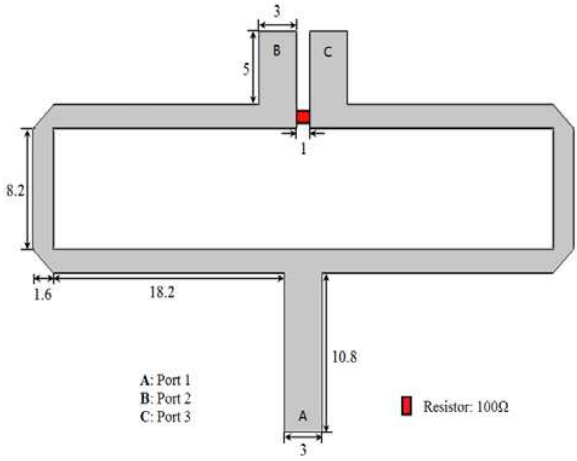

Figure 10. The configuration of the power divider. (Dimensions in mm).

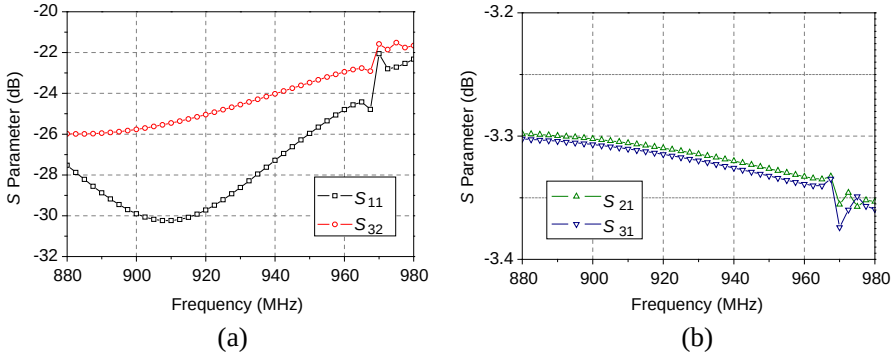

Figure 11. Simulated S parameter results of the power divider. (a) S_{11}/S_{32}. (b) S_{21}/S_{31}.

3.2.2. Power Divider

Wilkinson power divider is utilized in the antenna array as the feeding. According to the previous research [27], the Wilkinson power divider is implemented with an FR4 printed circuit board, as shown in Figure 10. The S parameters results of the power divider are shown in Figure 11. As shown in the figures, the divider achieves that the output from port 2 and port 3 are 3 dB loss from port 1 in the working band, with high isolation between them. In the proposed antenna array, the decoupling and matching network functions together with the power divider are as the feeding network. The feeding network is printed on the bottom side of the substrate.

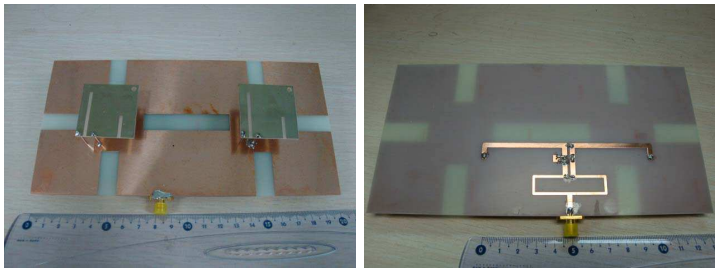

Figure 12. The pictures of the fabricated antenna array. (a) Top view. (b) Feeding network (Bottom side).

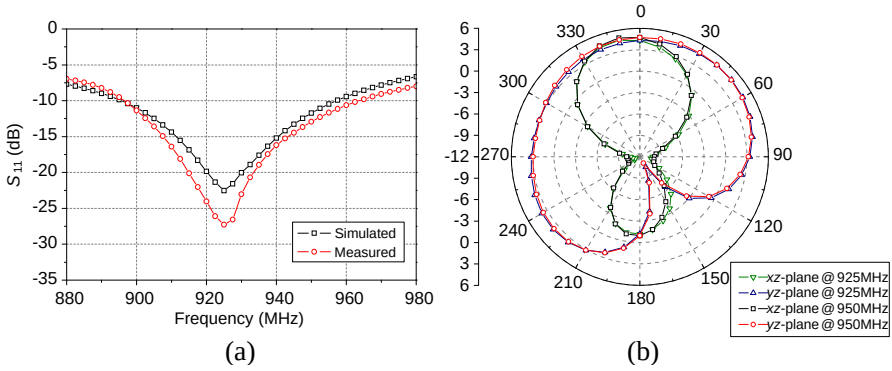

Figure 13. The results of the antenna array. (a) S_{11}. (b) Radiation pattern.

(a) (b)

Figure 14. The reading distance test. (a) Test scene. (b) Test tag.

Table 2. The comparison with other previous reader antennas.

	Overall size (mm^3)	Bandwidth (MHz)	Gain (dBi)
Proposed antenna	$200 \times 100 \times 20$	68	4.5
Antenna in [1]	$250 \times 180 \times 50$	11	7
Antenna in [2]	$260 \times 260 \times 35$	100	9.25
Antenna in [3]	$230 \times 230 \times 40$	55	4.7

4. ANTENNA ARRAY AND RESULTS

Figure 12 shows pictures of the fabricated antenna array. Two E-shaped patch antennas comprise the proposed antenna, and the feeding network is printed on the bottom side of the FR4 substrate. The overall size of the proposed antenna array is $200 \times 100 \times 20\,mm^3$.

The measured results of the antenna array are shown in Figure 13. The bandwidth of the antenna array is from 896 MHz to 964 MHz under the condition of S_{11} less than -10 dB, while the simulation result is from 895 MHz to 957 MHz. The error between these two results is about 9.6% which is mainly caused by the practical fabrication. The maximum gains are about 4.29 dBi and 4.72 dBi at 925 MHz and 950 MHz, respectively. The reading distance of the proposed antenna array is tested by UPM RAFLATAC tag, and the testing environment is shown in Figure 14. The max reading distance of the proposed antenna array is about 4.8 m alone z axis. Thus, the proposed antenna array can cover various RFID bands, and the gain meets the practical demands.

According to the results above, we compare the performance of

this antenna array with other previous UHF RFID reader antennas, as shown in Table 2. It is obvious that the proposed antenna array achieves better bandwidth in a smaller size. Besides, the antenna structure is more compact than the others. Thus the proposed antenna array could be called minimized and wideband.

5. STUDY OF ANTENNA ROBUSTNESS

5.1. Slots on the Patch

The dimensions of the slots on the patch are studied first, as shown in Figure 15. The lengths of the shorter and longer slots are named as L_1 and L_2, respectively. The width of these two slots is named as W_s. It is obvious that the longer slot and slot width are robust and will not affect the antenna performance greatly. The length of the shorter slot is relatively sensitive and could produce the frequency offset about 3 MHz when changing 2 mm.

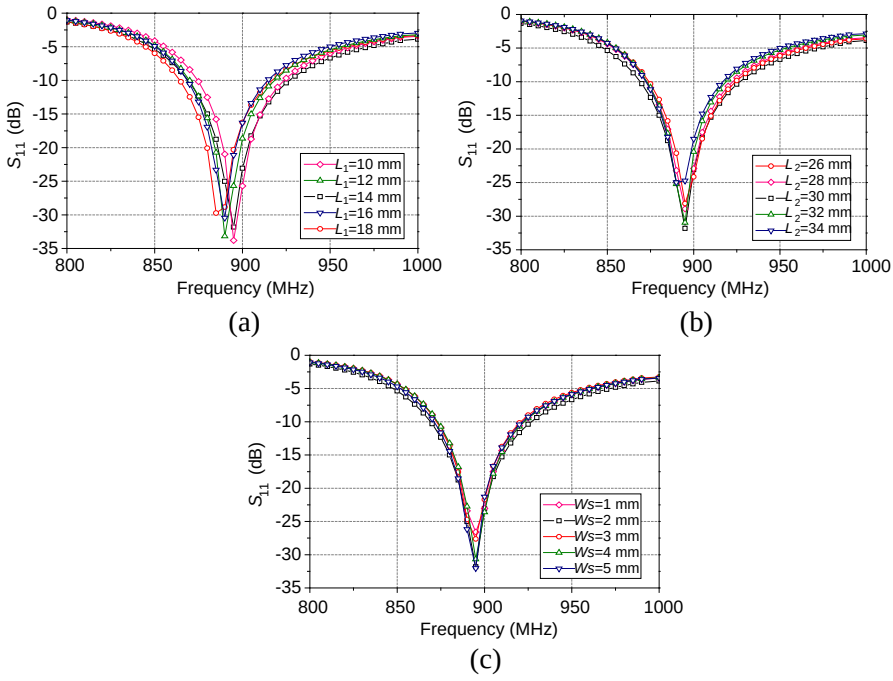

Figure 15. The effects of the slots on the patch. (a) Shorter slot. (b) Longer slot. (c) Slot width.

5.2. Slots on the Ground

Figure 16 shows the effects of the symmetric slots on the ground. The width and length of these same slots are named as W and L, respectively. The figures show that with increasing slot size, the resonance frequency is gradually downward. The input matching performance is improved first, and then decreased. Besides, the slot length is more critical for the input matching than the slot width. The resonant frequency would change about 50 MHz within 8 mm length change, while only 10 MHz when the width changes. $W = 12$ mm and $L = 29$ mm are selected as the better matching they achieved.

5.3. Height of the Patch

The effect of the patch height is shown in Figure 17 and the height named as H. The height of patch is the most sensitive parameter in the proposed antenna structure. It may cause about 20 MHz frequency offset when it changes 2 mm, while the antenna bandwidth would not be affected greatly. Considering the working center frequency, we choose $H = 20$ mm as the fabrication value.

After the analysis of the key parameters, we know the robustness of the proposed antenna. In general, the fabrication precision is higher than 0.1 mm. Thus the proposed antenna could be applied in the practical applications.

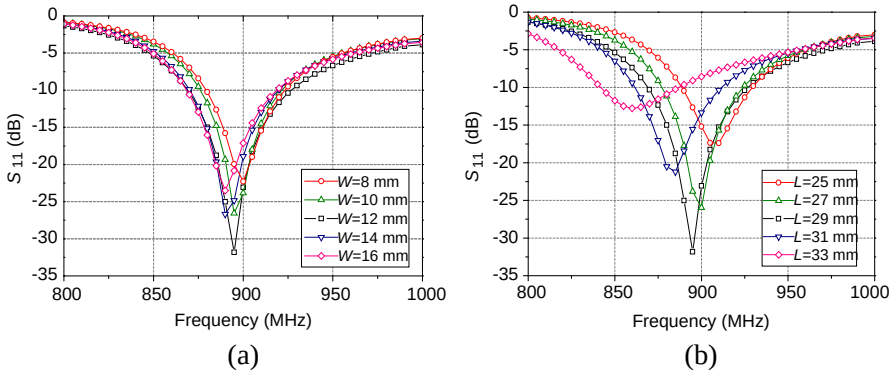

Figure 16. The effects of the slots on the ground. (a) Width. (b) Length.

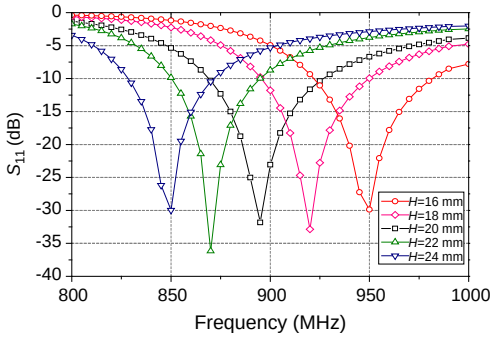

Figure 17. The effects of the patch height.

6. CONCLUSION

An antenna array for UHF RFID reader applications with wideband and high gain characteristics is presented in this paper. The antenna element is a compact E-shaped patch antenna with various miniaturizations and working around 920 MHz. Decoupling network and power divider are also designed for decoupling and feeding. The overall size of the reader antenna is $100 \times 100 \times 20\,\text{mm}^3$. The proposed antenna array is fabricated and measured. The measured bandwidth ranges from 896 MHz to 964 MHz, under the condition of voltage standing wave ratio less than 2. The average radiation gain is about 4.5 dBi in the working UHF band. Good agreement is achieved between the simulation and measurement. Besides, the key parameters are studied and prove its robustness. Therefore, the proposed antenna array could be suitable for UHF RFID reader applications.

ACKNOWLEDGMENT

This work is supported by the project 61072009 from the National Natural Science Foundation of China (NSFC), the 863 project 2011AA010201, Fundamental Research Funds for the Central Universities and the Fund of State Key Laboratory of Millimeter Waves, Southeast University (Grant No. K201209).

REFERENCES

1. Li, X. and J. Liao, "Eye-shaped segmented reader antenna for near-field UHF RFID applications," *Progress In Electromagnetics Research*, Vol. 114, 481–493, 2011.

2. Wang, P., G. Wen, J. Li, Y. Huang, L. Yang, and Q. Zhang, "Wideband circularly polarized UHF RFID reader antenna with high gain and wide axial ratio beamwidths," *Progress In Electromagnetics Research*, Vol. 129, 365–385, 2012.
3. Li, X. and L. Cao, "Microstrip-based segmented coupling reader antenna for near-field UHF RFID applications," *Microwave and Optical Technology Letters*, Vol. 53, No. 8, 1774–1777, Aug. 2011.
4. Li, X. and Z. Yang, "Dual-printed-dipoles reader antenna for UHF near-field RFID applications," *IEEE Antennas and Wireless Propagation Letters*, Vol. 10, 239–242, Apr. 2011.
5. Jamlos, M. F., A. R. B. Tharek, M. R. B. Kamarudin, P. Saad, O. Abdul Aziz, and M. A. Shamsudin, "Adaptive beam steering of RLSA antenna with RFID technology," *Progress In Electromagnetics Research*, Vol. 108, 65–80, 2010.
6. Chen, Z. N., X. Qing, and H. L. Chung, "A universal UHF RFID reader antenna," *IEEE Trans. Microw. Theory Tech.*, Vol. 57, No. 5, 1275–1282, May 2009.
7. Yang, F., X. X. Zhang, X. Ye, and Y. Rahmat-Samii, "Wide-band E-shaped patch antennas for wireless communications," *IEEE Trans. Antennas Propagat.*, Vol. 49, No. 7, 1094–1100, Jul. 2001.
8. Ang, B. K. and B. K. Chung, "A wideband E-shaped microstrip patch antenna for 5–6 GHz wireless communications," *Progress In Electromagnetics Research*, Vol. 75, 397–407, 2007.
9. Parikh, H., S. V. Pandey, and M. Sahoo, "Design of a modified E-shaped dual band patch antenna for Ku band application," *CSNT 2012*, 49–52, Rajkot, India, 2012.
10. Mallahzadeh, A. R., S. Es'haghi, and A. Alipour, "Design of an E-shaped MIMO antenna using IWO algorithm for wireless application at 5.8 GHz," *Progress In Electromagnetics Research*, Vol. 90, 187–203, 2009.
11. Lee, K. F., et al., "Experimental and simulation studies of the coaxially fed U-slots rectangular patch antenna," *IEE Proc. Microw. Antenna Propag.*, Vol. 144, No. 5, 354–358, Oct. 1997.
12. Eldek, A. A., A. Z. Elsherbeni, and C. E. Smith, "Dual-wideband square slot antenna with a U-shaped printed tuning stub for personal wireless communication systems," *Progress In Electromagnetics Research*, Vol. 53, 319–333, 2005.
13. Rafi, G. and L. Shafai, "Broadband microstrip patch antenna with V-slot," *IEE Proc. Microw. Antenna Propag.*, Vol. 151, No. 5, 435–440, Oct. 2004.
14. Tsay, W.-J. and J. T. Aberle, "Analysis of a microstrip

line terminated with a shorting pin," *Microwave Theory and Techniques*, Vol. 40, No. 4, 645–651, Apr. 1992.

15. Pedra, A. C. O., G. Bulla, P. Serafini, and A. A. A. Salles, "Shorting pins application in wide-band E-shaped patch antenna," *IMOC 2009*, 229–234, Belem, Brazil, 2009.
16. Chiou, T. W. and K. L. Wong, "Designs of compact microstrip antennas with a slotted ground plane," *IEEE APS 2001*, 732–735, Boston, USA, 2001.
17. Wong, K. L., J. S. Kuo, and T. W. Chiou, "Compact microstrip antennas with slots loaded in the ground plane," *IEE ICAP 2001*, 623–626, 2001.
18. Kuo, J. S. and J. B. Hsieh, "Gain enhancement of a circularly polarized equilateral-triangular microstrip antenna with a slotted ground plane," *IEEE Trans. Antennas Propagat.*, Vol. 51, No. 5, 1652–1656, Jul. 2003.
19. Chen, D. and C. H. Cheng, "A novel compact ultra-wideband wide slot antenna with via holes," *Progress In Electromagnetics Research*, Vol. 94, 343–349, 2009.
20. Yoon, W. S., J. W. Baik, and H. S. Lee, "A reconfigurable circularly polarized microstrip antenna with a slotted ground plane," *IEEE Antennas and Wireless Propagation Letters*, Vol. 9, 1161–1164, 2010.
21. Chung, Y., S. S. Jeon, D. Ahn, J. I. Choi, and T. Itoh, "High isolation dual-polarized patch antenna using integrated defected ground structure," *IEEE Microw. Wireless Comput. Lett.*, Vol. 14, No. 1, 4–6, Jan. 2004.
22. Chiu, C. Y., C. H. Cheng, R. D. Murch, and C. R. Rowell, "Reduction of mutual coupling between closely-packed antenna elements," *IEEE Trans. Antennas Propagat.*, Vol. 55, No. 6, 1732–1738, Jun. 2007.
23. Li, H., J. Xiong, and S. He, "A compact planar MIMO antenna system of four elements with similar radiation characteristics and isolation structure," *IEEE Antennas and Wireless Propagation Letters*, Vol. 8, 1107–1110, Oct. 2009.
24. Yang, L., M. Fan, F. Chen, J. She, and Z. Feng, "A novel compact electromagnetic-bandgap (EBG) structure and its applications for microwave circuits," *IEEE Trans. Microw. Theory Tech.*, Vol. 53, No. 1, 183–190, Jan. 2005.
25. Coetzee, J. C. and Y. Yu, "Closed-form design equations for decoupling networks of small arrays," *Electronics Letters*, Vol. 44, No. 25, 1441–1442, Dec. 2008.

26. Coetzee, J. C. and Y. Yu, "Design of decoupling networks for circulant symmetric antenna arrays," *IEEE Antennas and Wireless Propagation Letters*, Vol. 8, 291–294, May 2009.
27. Son, W. I., W. G. Lim, M. Q. Lee, S. B. Min, and J. W. Yu, "Design of compact quadruple inverted-F antenna with circular polarization for GPS receiver," *IEEE Trans. Antennas Propagat.*, Vol. 58, No. 5, 1503–1510, May 2010.